Student thesis series INES nr 297

Estimating leaf area index from satellite data in deciduous forests of southern Sweden.

Sandra Persson

2014
Department of
Physical Geography and Ecosystems Science
Lund University
Sölvegatan 12
S-223 62 Lund
Sweden

Sandra Persson (2014). Estimating leaf area index from satellite data in deciduous forests of southern Sweden.
Master degree thesis, 30 credits in *Physical Geography and Ecosystem Analysis*
Department of Physical Geography and Ecosystems Science, Lund University

Estimating leaf area index from satellite data in deciduous forests of southern Sweden.

Sandra Persson

Master degree thesis in
Physical Geography and Ecosystem Analysis

Supervisor:
Lars Eklundh

Department of Physical Geography and Ecosystems Science,
Lund university

Abstract

Leaf area index, LAI, is an important biophysical parameter in ecological modeling. It is a dimensionless ratio of leaf area per unit ground area. LAI controls many ecological processes like photosynthesis, evaporation and transpiration. To obtain LAI over large areas in a fast and convenient way the use of satellite data is important. Aim of the project was to determine if there is a relationship between LAI and red-, NIR reflectance and a couple of vegetation indices: Global Environment Monitoring Index (GEMI), Normalized Difference Vegetation Index (NDVI), Vegetation Phenology Index (VPI) and the two-band Enhanced Vegetation Index (EVI2). A related measure of LAI called effective LAI, L_e, which assumes a random foliage distribution, was estimated in the field with an optical instrument. The vegetation indices/reflectance was obtained from SPOT satellite data. Results showed that there is a linear relationship and good correlations, about 0.8, between L_e and the vegetation indices and NIR reflectance data. The red reflectance showed a weak relation to L_e. The relations between L_e and NIR reflectance, GEMI, VPI and EVI2 looked very similar indicating that it is the NIR reflectance that forms the relations. Three values were deviating from the linear relations but this could not be explained by difference in degree of understory vegetation or species composition of the stands. The deviation of two of the values could be due to thinning some time between the satellite image was recorded and the field measurements. The linear relationships could be used to get an estimate of LAI from the vegetation indices in deciduous forests of similar characteristics and within the range of L_e values as in this study.

Sammanfattning

Bladyteindex (eng. Leaf Area Index, LAI) är en viktig biofysisk parameter inom ekologisk modellering. Den är en dimensionslös kvot av lövytan per markenhet. LAI kontrollerar många ekologiska processer såsom fotosyntes, evaporation och transpiration. Man använder satellitdata för att uppskatta LAI på ett snabbt och lättillgängligt sätt. Syftet med projektet var att bestämma om det finns ett förhållande mellan LAI och röd-, nära infraröd (NIR) reflektans samt några vegetationsindex: Global Environment Monitoring Index (GEMI), Normalized Difference Vegetation Index (NDVI), Vegetation Phenology Index (VPI) och Enhanced Vegetation Index av två våglängdsband (EVI2). Ett relaterat mått till LAI kallat effektiv LAI, L_e, vilket förutsätter att lövverket är slumpmässigt fördelat, uppskattades i fält med ett optiskt instrument. Vegetationsindexen/reflektansen kom från SPOT satellit data. Resultaten visade att det finns ett linjärt samband med bra korrelationer, ungefär 0.8, mellan L_e och vegetationsindexen samt med reflektans i NIR. Reflektans i det röda våglängdsområdet visade svagt samband med L_e. Sambanden mellan L_e och reflektans i NIR, GEMI, VPI och EVI2 såg väldigt lika ut vilket visar att det är reflektansen i NIR som ligger till grund för sambanden. Tre värden avvek från de linjära sambanden, men det kunde inte förklaras med skillnad i grad av undervegetation eller olika arter i bestånden. Avvikelsen för två av värdena kan bero på gallring någon gång mellan tagningen av satellitbilden och fältmätningarna. De linjära sambanden skulle kunna användas för att få en uppskattning av LAI från vegetationsindex i lövskogar med liknande egenskaper och inom samma intervall av L_e-värden som i denna studie.

Table of contents

1. Introduction

Leaf area index, LAI, is an important biophysical parameter controlling many ecological processes like photosynthesis, evaporation and transpiration. LAI is a dimensionless ratio of the leaf area per unit ground area. It directly controls the vegetation gas exchange and carbon gain or gross primary production (GPP) of an ecosystem (Schulze et al., 1994) and is used in many ecological modeling applications. It is a key parameter in models that simulate the terrestrial carbon balance. Remote sensing with satellites can be used to estimate LAI over large areas, when using field measurements of LAI can be very expensive and time-consuming work. By monitoring LAI over time one could get information about how changes in climate affect the productivity of ecosystems. Since the LAI will be affected if a forest is subject to stress, like insect attacks, drought or other environmental changes, it can be an indicator of the health of forests. To get information about the changes and health of ecosystems on a regional scale the possibility to estimate LAI from satellite data is important.

The sensor on satellites that monitors vegetation records the radiance from the earth in different wavelength bands. The radiance from different surfaces can then be converted to the reflectance of the surfaces. For vegetation the red and near infra-red (NIR) wavelengths are especially interesting because leaves absorb a lot of energy in the red wavelengths, due to photosynthesis, while they reflect a lot of light in NIR, due to their inner structure. This reflectance in the red and NIR part of the light spectrum can then be used to estimate biophysical parameters like LAI and fraction of Absorbed Photosynthetically Active Radiation (fAPAR).

The different wavelength bands can be arithmetically combined to form vegetation indices, which are designed to enhance the vegetation. The most commonly used vegetation index is the Normalized Difference Vegetation Index (NDVI), which has a non-linear relationship to LAI (Turner et al., 1999). A problem with the NDVI-LAI relationship is that NDVI saturates at higher values of LAI (Turner et al., 1999). Another

problem is that NDVI is sensitive to scattering by atmospheric aerosols (Ben-Ze'ev et al., 2006).

Today there are two common methods to estimate LAI from satellite data. One is to use a physically based radiative transfer model that simulates the radiation inside the canopy. By letting the model change different parameters related to the reflectance properties of the canopy, like LAI, the simulated canopy reflectance changes until it agrees with the reflectance from satellite data. Then LAI is obtained from the parameter set that agreed best. Problems with this method are that different combinations of the parameters can give the same reflectance (Combal et al., 2002). Another problem is that to choose the input data for the different parameters are complicated and often relies on experimental data (Gonsamo et al., 2010), which makes the method not applicable on large scales. The other method is to find empirical/statistical relationships between the satellite reflectance/vegetation indices and LAI. This method is simpler and could be used to map LAI on large scales, but it is not based on physical relationships like the radiative transfer models.

Aim

Aim of the project is to use the empirical approach and determine a relationship between LAI and some vegetation indices, which were developed to overcome the limitations of NDVI. The indices will be tested against LAI of deciduous forests in southern Sweden, where not many studies like this have been done. The first index to be tested is the Global Environment Monitoring Index (GEMI) which has been developed to be less sensitive to atmospheric scattering than NDVI. The second is the two-band Enhanced Vegetation Index (EVI2) that should not saturate as much as NDVI at higher LAI values. The third is the Phenology Vegetation Index (VPI), which is a new, physically based index that has never been tested before against field measurements of LAI but in theory should have a linear relationship to LAI.

2. Background

To get energy for photosynthesis the leaves absorb a lot of light in the visible wavelengths (0.4-0.7 μm), especially in the red and blue region of the spectrum. Due to the inner structure of leaves they have high reflectance in the near-infrared (NIR) wavelengths (0.75-1.35 μm). The sharp rise in reflectance between the red and NIR wavelengths is called the red edge. In the shortwave infrared (SWIR) part of the spectrum the water content of leaves becomes the dominating factor controlling leaf reflectance with strong absorption in some wavelengths. It is the unique spectral signals from the vegetation that makes it useful to estimate different properties of the vegetation, such as LAI, fAPAR and chlorophyll and nitrogen content using remote sensing.

2.1. Leaf area index and effective LAI

There are different definitions of LAI. A common definition is half the total leaf area per unit ground surface area (Chen and Black, 1992). A related measure of LAI is effective LAI, L_e, (Black et al., 1991). It was developed to be used in the estimation of shortwave and longwave irradiance of a Douglas-fir forest stand (Black et a., 1991). L_e can be estimated from measurements of the radiation below and beneath the canopy using an optical instrument, which is practical and easy to do compared to the traditional method of collecting leaves in litter traps to estimate LAI. L_e is not the true LAI, though, because in the calculation of L_e a random spatial distribution of leaves is assumed, when in reality leaves are often aggregated on top of each other. Also, when measuring the above and below canopy radiation not only leaves but also non-photosynthetic material, like stems, branches and fruit, will be included as part of the "LAI".

L_e originates from gap fraction theory, which describes the probability, $P(\theta)$, that a beam of incoming radiation from the zenith angle, θ, is not intercepted by the canopy. $P(\theta)$ depends on the foliage density, μ (m^2m^{-3}), the fraction of foliage projected toward θ, $G(\theta)$, and the path length that radiation will travel through the canopy, $S(\theta)$ (m):

(1) $$P(\theta) = \exp[-G(\theta)\cdot\mu\cdot S(\theta)]$$

The probability of non-interception, $P(\theta)$, is also called the gap fraction. Rearranging (1) so $G(\theta)$ and μ end up on the left side you get the contact frequency, $K(\theta)$ (m^{-1}) (Miller, 1967):

(2) $$G(\theta)\cdot\mu = - \ln(P(\theta))/S(\theta) = K(\theta)$$

The contact frequency is the number of contacts per meter a probe would make that goes through the canopy at zenith angle, θ. The average foliage density according to Miller (1967) is:

(3) $$\mu = 2 \int -\ln(P(\theta))/S(\theta)\cdot\sin\theta d\theta, \quad 0 \leq \theta \leq \pi/2$$

The average foliage density is equal to the leaf area index, multiplied with the height of the canopy, z; μ=LAI·z. The path length is equal to the height of the canopy divided by the cosine of the zenith angle; $S(\theta)=z/\cos\theta$. Putting these relations into (3) cancels the height z, and yields L_e as the logarithm of the gap fractions integrated over all hemispherical view zenith angles (Black et al., 1991):

(4) $$L_e = - 2 \int \ln(P(\theta))\cdot\cos\theta\cdot\sin\theta d\theta, \qquad 0 \leq \theta \leq \pi/2$$

Important assumptions to the above formulas are that the canopy foliage is randomly distributed and the foliage elements are small. In the above equations the azimuthal angle is not taken into consideration, which means that the gap fraction is assumed as constant over all azimuthal angles.

Studies have shown that the estimation of L_e using optical instruments that measures the radiation above and below the canopy, such as the LAI-2000 Plant Canopy Analyzer used in this study (see Material and Methods section below), underestimates the true LAI (Chason et al., 1991; Cutini et al., 1998). This is because of the assumption of random foliage distribution and for deciduous forests the underestimation may be about 26.5% (Cutini et al., 1998). To obtain LAI from L_e different correction factors for the woody material, clumping and aggregation of leaves are used. In temperate deciduous forests of

southern Sweden these correction factors have proven to almost cancel each other out why L_e in these forests can be approximated as the true LAI (Eriksson et al., 2005). Studies have also shown that L_e and LAI are linearly related to each other, for both deciduous and coniferous forests (Chason et al., 1991; Cutini et al., 1998; Rautiainen et al., 2003).

2.2. Vegetation indices

In remote sensing the reflectance from the vegetation in different wavelength bands is influenced by many factors like atmospheric and topographic effects, different soil background and variations in sun and viewing angles. Some of these effects can be removed by using arithmetic combinations of different bands. The big difference in red and NIR reflectance (the red edge) of vegetation is utilized to form the most commonly used vegetation index in remote sensing, NDVI:

$$\text{NDVI} = (\rho_{\text{NIR}} - \rho_{\text{red}}) / (\rho_{\text{NIR}} + \rho_{\text{red}}) \quad (5)$$

Values of NDVI ranges between –1 to 1 and for vegetation the values are between 0.1 and 0.8 because of the high reflectance in NIR. Clouds, water and snow have higher red reflectance and therefore negative values, while rock and bare soil have almost the same reflectance in both red and NIR and thus have NDVI values of about 0. NDVI is very useful because it has a nearly linear relation to fAPAR (Asrar et. al., 1984). The fAPAR can be multiplied with the photosynthetically active radiation (PAR), which is the visible light with wavelengths from 0.4 to 0.7 μm, to get the absorbed PAR. The absorbed PAR is the energy used for photosynthesis and therefore it regulates the conversion of energy to biomass. By using a light use efficiency model (Monteith, 1972) the Gross Primary Productivity (GPP) can be calculated from the absorbed PAR.

Earlier studies have shown that there is a relationship between NDVI and LAI. For example a significant linear correlation was found between NDVI, calculated from Landsat TM data, and LAI for deciduous forests in southern Scania, Sweden (Eklundh et al., 2003). Another study performed in mixed and coniferous forests showed a good relationship between LAI and NDVI with a cubic polynomial fit (Turner et al., 1999).

There are some limitations to NDVI. It is sensitive to scattering from aerosols (Ben-Ze'ev et al., 2006) and changes dependent on soil reflectance background (Bausch, 1993). A problem is also that NDVI saturate when LAI reaches a level of 3 to 5 m^2m^{-2} (Turner et al., 1999) in dense vegetation, for example in the Amazon rainforest (Huete et al., 2002). Pinty and Verstraete (1992) proposed a new index called Global Environment Monitoring Index (GEMI), which should be less sensitive to effects of atmospheric scattering than NDVI. The index is defined as follows:

(6) $$GEMI = \eta(1-0.25\eta) - (\rho_{red} - 0.125) / (1-\rho_{red}),$$

where $$\eta = [\, 2(\rho_{NIR}^2 - \rho_{red}^2) + 1.5 \cdot \rho_{NIR} + 0.5\rho_{red}] / [\rho_{NIR} + \rho_{red} + 0.5].$$

Another vegetation index, which also was developed to overcome the limitations of NDVI, is the Enhanced Vegetation Index, EVI. This index includes the blue wavelength to compensate for the scattering of the atmosphere and a soil-adjustment factor, L:

(7) $$EVI = G\,(\rho_{NIR} - \rho_{red}) / (\rho_{NIR} + C_1\rho_{red} - C_2\rho_{blue} + L)$$

G is a gain factor and C_1 and C_2 are coefficients correcting for the influence of aerosols in the atmosphere. In the MODIS EVI algorithm the coefficients are C_1=6, C_2=7.5, L=1 and G=2.5. EVI does not saturate at higher biomass levels like NDVI but stays sensitive to changes even when LAI reaches high values (Houborg et al., 2007). This index will need the blue band, which some sensors on satellites do not have. Therefore an alternative to the EVI that does not include the blue band, called EVI2, was developed by Jiang et al. (2008):

(8) $$EVI2 = 2.5(\rho_{NIR} - \rho_{red})/(\rho_{NIR} + 2.4\rho_{red} + 1))$$

Studies have shown that EVI2 and EVI are equivalent (Jiang et al., 2008; Rocha and Shaver, 2009). EVI2 is less sensitive to background reflectance and better at resolving

differences in surface greenness than NDVI (Rocha and Shaver, 2009). The relationship between EVI2 and LAI has been tested on crops using a non-linear semi-empirical formula based on Beer's law (Liu et al., 2012). The LAI obtained from the formula showed good agreement with the estimated L_e (Liu et al., 2012).
A recently developed index that was also tested in this study is the phenology vegetation index, VPI (Jin, unpubl.). This was developed to better describe the vegetation phenology in high northern latitudes:

(9) $VPI = - G*\ln[(M - DVI)/M]$

G is a gain factor, $M = NIR_\infty - Red_\infty$ is the difference between NIR and red reflectance for infinitely thick vegetation which can be obtained from long-term measurements and DVI = NIR – Red. VPI is a physically based vegetation index originating from a modified version of Beer´s law. In theory it is suppose to have a linear relationship with LAI (Jin, unpubl.) but this has never been tested with actual measurements of LAI.

3. Materials and methods

3.1. LAI-2000 Plant Canopy Analyzer

The measurements of the canopy gap fraction were conducted by using the LAI-2000 Plant Canopy Analyzer (PCA) (Li-Cor, Inc.). During measurements, two separate sensors are used. The sensors have five different detectors in concentric rings that each views a portion of the hemisphere: 0-13°, 16-28°, 32-43°, 47-58° and 61-74°. The measurements are done by placing one logging sensor out in an open field recording the above canopy irradiance and taking samples with the other sensor below the forest canopy. To get the gap fraction the below canopy readings are divided by the above canopy readings. There are four important assumptions with this method. First the foliage is assumed to be black, i.e. there is no scattering of the direct incoming light. To reduce the scattering of light the PCA has a filter, which only permits wavelengths from 320 nm to 490 nm to pass. At wavelengths below 490 nm the scattering of light by foliage is minimal (LAI-2000 Plant Canopy Analyzer, Instruction manual, Li-Cor Inc., 1990). The second assumption is that the foliage is randomly distributed. In reality leaves are oriented around the branches, and

especially for conifer trees the needles are not situated randomly in the canopy. Thirdly the foliage elements are assumed to be small, which is true when holding the sensor at a distance of at least four times the leaf width. The fourth assumption is that the foliage is randomly oriented with respect to the azimuthal angle.

3.2. Study sites

Measurements were carried out in 15 deciduous forest stands in Skarhult and Fulltofta in the province of Scania, Sweden (Figure 1, Appendix). The areas of Skarhult and Fulltofta have an average temperature of –2 - 0°C in January and 16-18°C in July and yearly precipitation of 700 mm. In August and September of 2013, when the measurements of L_e were conducted, the weather conditions were quite normal for this area with an average temperature of 17°C in August and 13°C in September. The amount of precipitation in August was also normal, 50-75 mm, but in September it was a little drier with a precipitation of 50 mm which is about 75% of the normal amount. During the month before I started my measurements, July, there had been a long drought. The average temperature of 17°C had not been much higher than usual, but the precipitation of 25 mm was about 50% of the normal amount in July. The satellite image used in this study is from June 6, 2012. In the beginning of June this year it was wet and cold in the study sites. During the month before, May 2012, the weather had varied with quite low amount of precipitation, 25 mm, which were about 50% of the normal amount, and an average temperature of 13°C (SMHI, 2014).

The deciduous forest stands were chosen to be of different densities so that I would get a wide range of L_e values. Thus stands with both dense and more open canopies were chosen. Measurements were only conducted in deciduous forests because the leaves in these forests are closer to being randomly distributed, which is one of the assumptions mentioned earlier, as oppose to a coniferous forest. They differed in species composition, understory vegetation and canopy closure. The degree of understory was estimated into two categories: little or much. The stands with much understory had the whole ground covered with vegetation, like ferns and bushes. In the stands classified as having little understory the understory vegetation consisted of some mosses and low grasses or no a vegetation at all. Eleven of the stands were homogeneous consisting of just one single

species, *Fagus sylvatica* (common beech) or *Quercus robur* (pedunculate or English oak), while the other stands consisted of a mixture of deciduous species like *Fagus sylvatica***,** *Betula pendula* (silver birch) and *Quercus robur*.

3.3. Field measurements

The measurements were conducted from August 16 until October 1 in 2013, when the trees were fully in leaf. The dates and L_e values can be seen in Figure 2 in Appendix. Almost all of the leaves were still green even at the end of this period of measurements. The weather was overcast to avoid scattering of direct sunlight to affect the measurements. The logging sensor was placed in big open places with a distance of at least 3.5 times the height of the nearest tree and less than 2 km from the forest stands. It was set to record the radiation every 15 seconds. Compass direction of the sensor was noted. In each forest stand 30 recordings were taken with the other sensor in three transects (ten in each transect) in a 30×30 m square (15 m between each transect), with the sensor held in the same compass direction as the logging sensor. A 180° view cap was used on both sensors to avoid the operator to be included in the measurements. GPS position was recorded for each forest stand in the middle of the square.

3.4. Calculations of effective LAI

The gap fractions and L_e was calculated using the C2000 program included in the equipment. First the path lengths (which are equal to $1/\cos\theta_i$ because the height z is cancelled out later in the calculations (see theory section) divide the logarithms of the gap fractions for each of the five viewing angles to get the contact frequencies, $K(\theta_i)$, for each angle of view, θ_i (eq. 2). The angles of views are the middle values of the five portions of the hemisphere that the detectors in the rings see: 7°, 23°, 38°, 53° and 68°. The contact frequencies are averaged over the 30 gap fractions calculated for each forest stand. L_e is then calculated using equation (4) by summing up the product of the averaged contact frequencies and the sinus of θ_i for every angle of view:

$$(10) \qquad L_e = 2 \sum K(\theta_i)\cdot\sin\theta_i\cdot\Delta\theta_i, \qquad 1 \le i \le 5$$

In the calculations it is possible to exclude certain rings to get a better estimation of LAI. Cutini et al. (1998) found that the value of L_e came closer to the true LAI when excluding the fifth ring. Since the leaves are mostly situated in the upper part of the canopy and the fifth sky sector includes mostly stems (Cutini et al., 1998) I calculated L_e both with and without the fifth ring to see if it would have any effect on my results.

3.5. Satellite data- radiometric correction and calculations of vegetation indices

The satellite data were obtained from the Saccess database, Swedish National Land Survey. The satellite image was from the High Resolution Geometric (HRG) sensor on SPOT-5 recorded at June 6, 2012. The image has four different wavelength bands- green, red, near infrared (NIR) and short-wave infrared (SWIR) (Table 1). The data was supplied as orthorectified and geometrically corrected to the SWEREF99 projection.

Table 1. The four wavelength intervals and spatial resolution of the bands from SPOT-5.

Band	**Wavelengths (μm)**	**Spatial resolution (m)**
Green	0.50-0.59	10
Red	0.61-0.68	10
NIR	0.78-0.89	10
SWIR	1.58-1.75	20

A radiometric correction was done to the data. The digital numbers (DN) were converted to spectral radiance, L_λ, for each wavelength band, λ, using the following formula (Astrium, 2013):

(11) $L_\lambda = DN/G + B$

Where G is gain and B is bias. For all the bands the biases were zero and the gains (in units of $Wm^{-2}Sr^{-1}\mu m^{-1}$) were 2.903582, 3.680142, 1.295663 and 10.585723 for the green, red, NIR and SWIR band respectively. The planetary reflectance, ρ_p, was calculated as (U.S. Geological Survey, 2011):

(12) $\rho_p = \pi \cdot L_\lambda \cdot d^2/(E_{sun\lambda} \cdot \cos\theta)$

The reflectance, ρ_p, is unitless, d is the Earth-Sun distance in astronomical units, $E_{sun\lambda}$ is the mean solar exo-atmospheric spectral irradiance in $Wm^{-2}\mu m^{-1}$ and θ is the solar zenith angle.

Radiometric correction and calculations of vegetation indices were done in the GIS software Idrisi Selva. The vegetation indices were calculated using equations 5, 6, 8 and 9 for NDVI, GEMI, EVI-2 and VPI respectively. The factor M (difference between NIR and red reflectance for infinitely thick vegetation) in the equation for VPI (eq. 9) was estimated by taking the largest difference between NIR and red reflectance in the SPOT-5 image (0.45) and adding 0.05 to this value. Thus M was set to 0.5. The gain factor, G, was set to 1.

The GPS points that were recorded in the geographic coordinate system WGS84 were converted into SWEREF99 projection to match the satellite data. The average value of a 3×3 window, with the GPS-point situated in the middle, for the vegetation indices and red- and NIR reflectance was calculated. Thus the average value of vegetation index/reflectance of the 30×30 m square in the satellite image corresponded to the average L_e value of the 30×30 m square in the field measurements.

Correlations and relations between L_e and the vegetation indices/reflectance were calculated using Matlab 7.6.0. To be able to see if the understory vegetation had an influence on the reflected signal a figure showing the different degree of understory cover was also made (Figure 7). Since different species might have different biochemical properties of leaves, like pigment concentrations, that might affect the reflectance (Blackburn et al., 1991) an additional figure was made showing the different species compositions of the stands (Figure 8).

4. Results

The correlation between the reflectance or vegetation indices and L_e did not differ much whether all rings or all rings but the fifth were used in the calculation of L_e (Table 2).

Table 2: The vegetation indices and reflectance and their correlation to L_e with all rings of the PCA included and without the fifth ring. Significant correlations in bold (Significance level is 0.05).

Vegetation index/Reflectance	**Correlation (all rings)**	**Correlation (without ring 5)**
Red	-0.50	-0.49
NIR	**0.81**	**0.80**
VPI	**0.79**	**0.78**
GEMI	**0.83**	**0.83**
EVI2	**0.84**	**0.83**
NDVI	**0.84**	**0.84**

All correlations are significant with a p-value much lower than 0.05, except for the red reflectance and L_e relation that had a p-value of 0.057, which is very close to being significant though. The correlation of –0.50 between L_e and red reflectance indicate a weak relationship between L_e and red reflectance (Table 2) and the values are scattered (Figure 1). There appears to be a grouping between the two sites, Fulltofta and Skarhult; the red reflectance is generally lower for Fulltofta than for Skarhult (Figure 1).

The correlation is higher, 0.81, between the NIR reflectance and L_e (Table 2) and there seems to be a linear relation (Figure 2). The grouping between the sites that can be seen in Figure 1 of the relation between red reflectance and L_e cannot be seen for the NIR reflectance (Figure 2). One can also see in Figure 2 that three points, with L_e values of 3.77 to 4.15 and NIR reflectance values of 0.41 to 0.43 are deviating from the rest.

The relationship between VPI, GEMI, EVI2 and L_e (Figure 3-5) is similar to the relation between NIR reflectance and L_e (Figure 2), and in Figure 3-5 there are the same three deviating points.

The relationship between NDVI and L_e indicates a linear relation too, with the highest correlation next to EVI2, 0.84 (Figure 6, Table 2).

In order to identify if the three deviating points in Figure 2-5 are related to the degree of understory cover or species composition of the stands two additional figures were made. Figure 7 shows the plots with a high understory cover and Figure 8 the species present in the stands. There is no indication that the difference in reflectance for the three deviating points is due to species composition or understory cover. The two figures show the relationship for NIR reflectance and L_e but the pattern is the same when the figures of the vegetation indices and their relation to L_e are used.

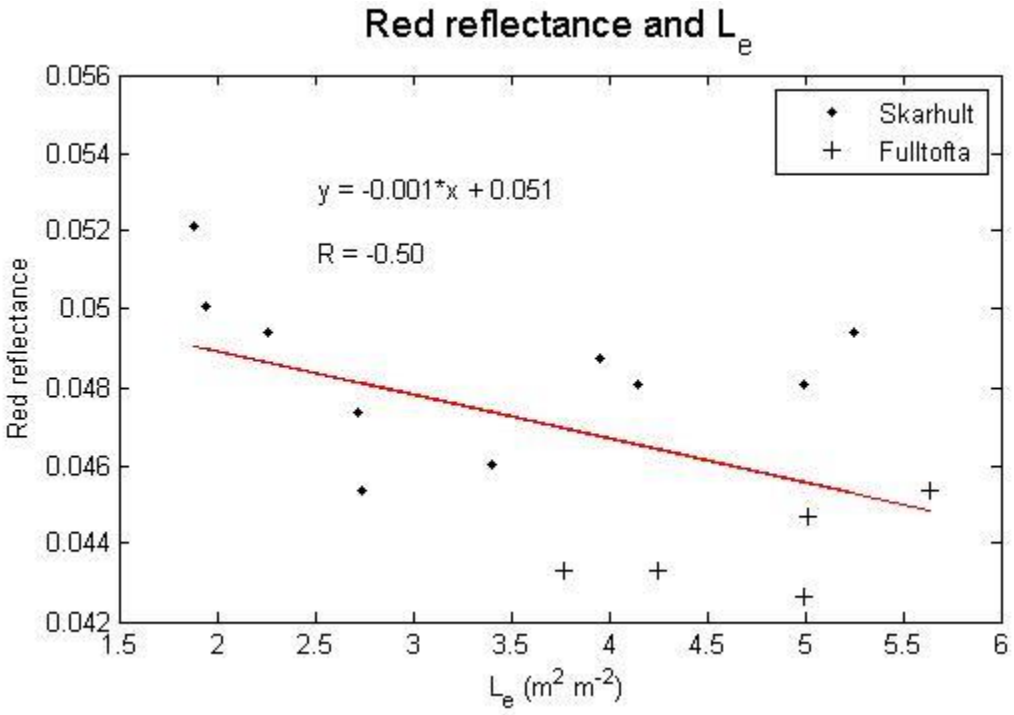

Figure 1. Relationship between red reflectance and L_e for the 15 plots in Skarhult and Fulltofta.

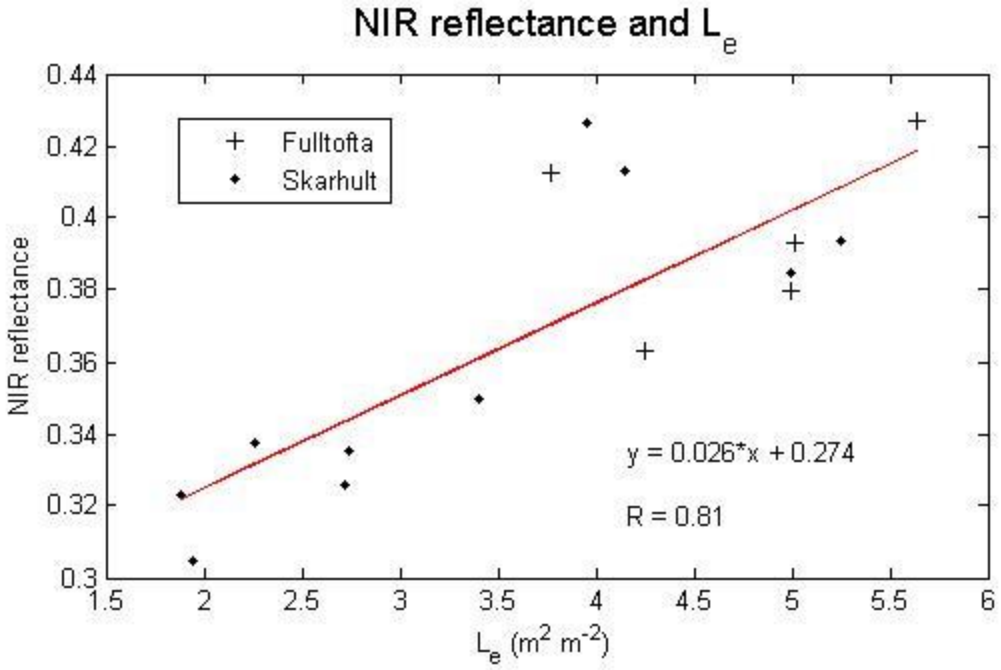

Figure 2. Relationship between NIR reflectance and L_e for the 15 plots in Skarhult and Fulltofta.

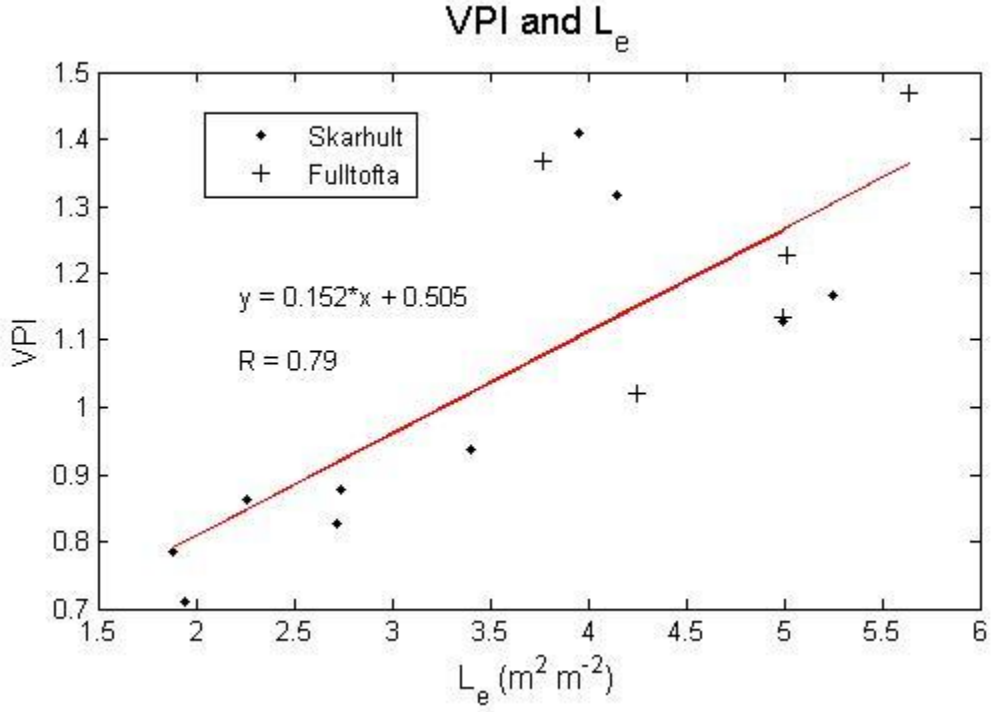

Figure 3. Relationship between VPI and L_e for the 15 plots in Skarhult and Fulltofta.

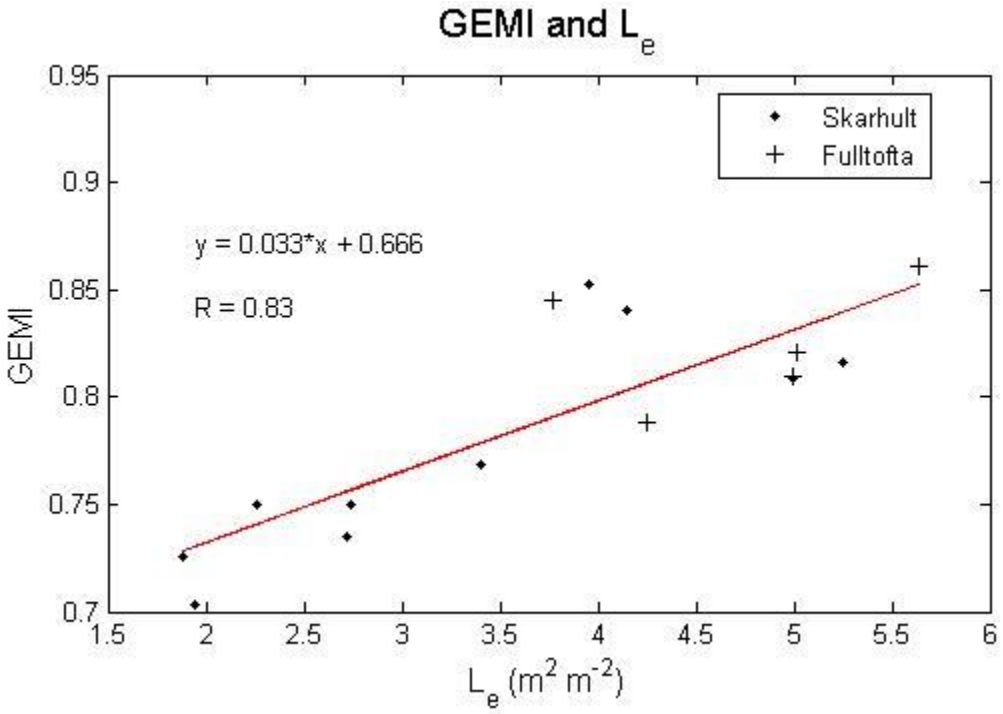

Figure 4. Relationship between GEMI and L_e for the 15 plots in Skarhult and Fulltofta.

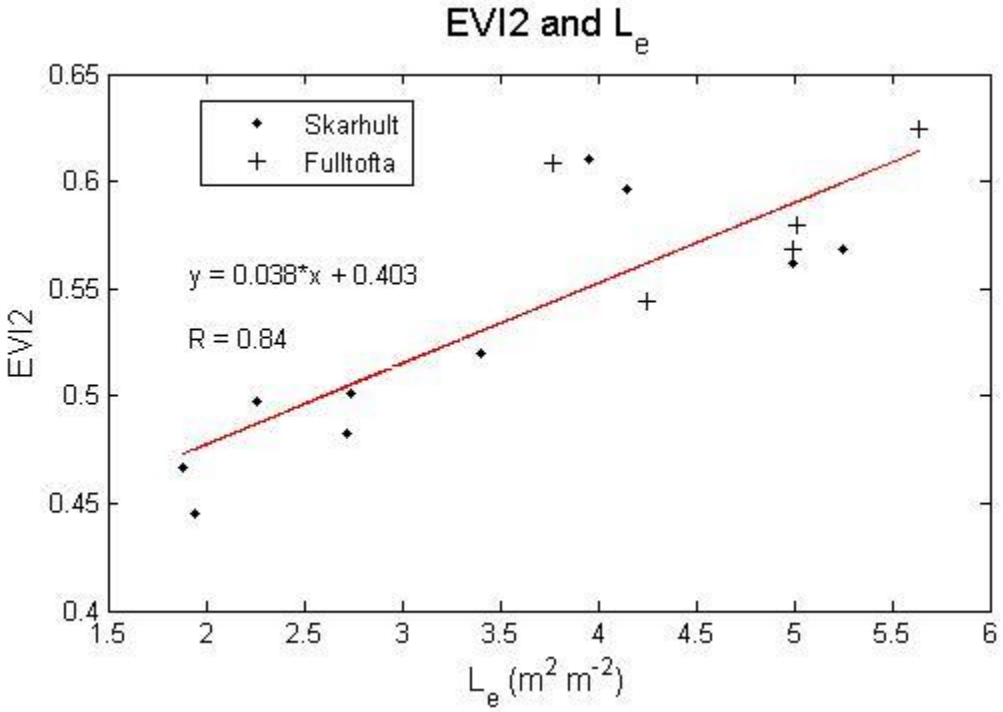

Figure 5. Relationship between EVI2 and L_e for the 15 plots in Skarhult and Fulltofta.

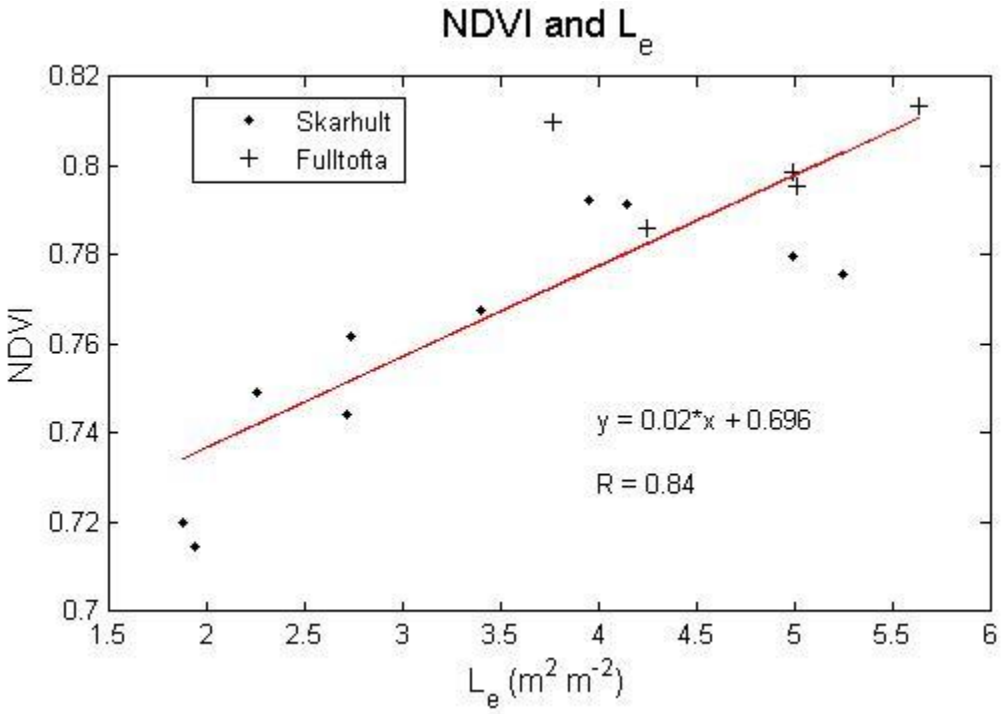

Figure 6. Relationship between NDVI and L_e for the 15 plots in Skarhult and Fulltofta.

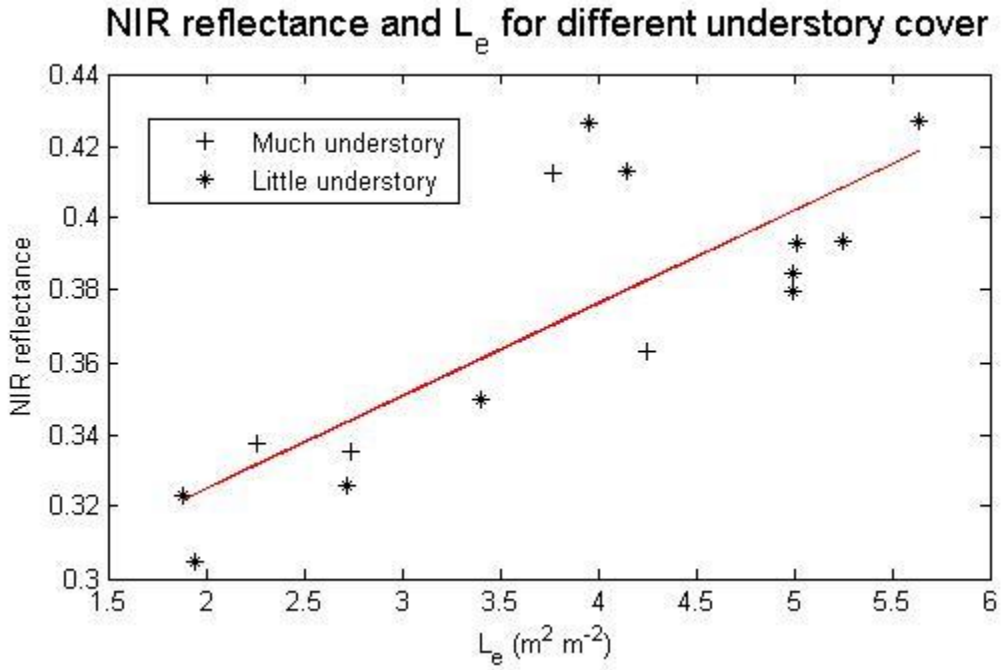

Figure 7. Relationship between NIR reflectance and L_e, showing the difference in understory cover, much or little, of the 15 plots.

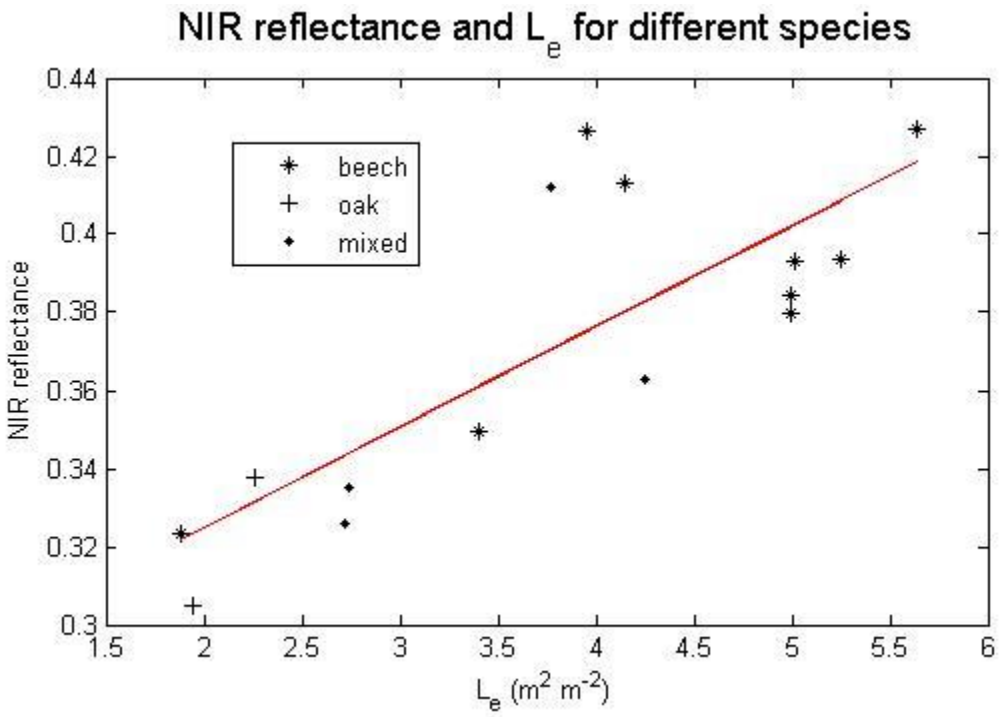

Figure 8. Relationship between NIR reflectance and L_e, showing the different species compositions of the plots.

5. Discussion

All the vegetation indices and the NIR reflectance in this study indicated a linear relationship to L_e with almost the same correlation, around 0.80 (Table 2). The correlations obtained in this study between NDVI, GEMI and NIR reflectance to L_e are higher than what has been estimated before by Eklundh et al. (2003) in deciduous forests. They got correlations of 0.62, 0.55 and 0.54 for NDVI, GEMI and NIR reflectance respectively, compared to 0.84, 0.83 and 0.81 (Table 2) in this study. In that study they had a higher number of deciduous plots where L_e was estimated, 42 compared to 15 in this study. Since I had a quite low amount of test plots some caution should be taken when interpreting my results and in comparing my results to others.

Both NIR reflectance and NDVI have a non-linear relationship to LAI (e.g. Turner et al., 1999; Soudani et al., 2006) but in this study NDVI has the best linear correlation (alongside with EVI2) of all vegetation indices. This could be because of the limited range of LAI values in this study; L_e reaches the highest value of about 5 m^2m^{-2}. At these values the relation seems to be linear and a plateau or saturation has not yet been reached. Saturation usually happens for LAI values around 3-5 m^2m^{-2} (Turner et al., 1999). When using a broader range of LAI from 1 to 13 m^2m^{-2}, a cubic polynomial has been shown to better fit the relationship (Turner et al., 1999).

When it comes to EVI2 a study performed in tundra region showed a significant linear LAI-EVI2 relation but the range of LAI values was very low, about 0 to 2 (Rocha and Shaver, 2009). On the other hand Liu et al. (2012) found good non-linear relations between LAI and EVI2 for crops, with the same range of L_e values as in this study.

For NIR reflectance, VPI, GEMI and EVI2 the figures are very similar, and all have the same three deviating points (Figure 2-5). In two of these points it is likely that thinning has occurred in the stand after the satellite image was recorded in 2012, before my measurements in 2013. Branches left lying on the ground in these stands indicated thinning. This would mean that the LAI's of these stands were higher in 2012 than in 2013 and thus the vegetation indices and NIR reflectance have higher values according to the satellite data than what the values of L_e indicate. In the third plot that is deviating there was a high cover of understory vegetation which can have an impact on the

reflected signal to the satellite sensor (Eriksson et al., 2006). Since the measurements with the PCA only include the canopy and not the understory the sensor sees more vegetation than the PCA, and thus LAI or L_e does not match the reflected signal. This is especially important when the LAI of the forest is below 3; then more of the understory vegetation is seen by the satellite (Eriksson et al., 2006). The L_e of this plot is not below 3, but close enough 3.77 m^2m^{-2}, and thus the understory might have an influence on the reflected signal. Looking at Figure 7, this explanation of why the point is deviating is not satisfactory because there are other points with much understory and even lower values of L_e that do not deviate from the other points. The species composition of the stands did not help in explaining why any point was deviating either (Figure 8).

The red reflectance indicates a weak non-linear relation to L_e (Figure 1). There is a weak negative correlation of –0.50 that is close to being significant ($p=0.057$). In theory the red reflectance should have a non-linear relation to LAI. The lower values of red reflectance for the Fulltofta site (Figure 2) could be due to atmospheric disturbances like haze in the satellite image, though it is not visible.

VPI, GEMI, EVI2 and their relation to L_e seem to be originating from the NIR reflectance, because when looking at the figures they are almost similar (Figure 2-5). The relation between NDVI and L_e differs from the other vegetation indices though (Figure 6). The two plots where it was probable that thinning had occurred do not deviate that much as in the other figures. This could perhaps be due to the fact that NDVI is worse at resolving changes in surface greenness than for example EVI2 (Rocha and Shaver, 2009).

There was no difference when using four or five rings when it came to the relation between L_e and vegetation indices/reflectance (Table 2). The only difference was that the values of L_e were higher when using only the four upper rings in the calculation. This is in agreement with Cutini et al. (1998) who also concluded that the underestimation of LAI, due to the assumption of random foliage distribution, becomes smaller and thus the value of L_e closer to the real LAI when excluding the fifth ring.

Different sky conditions can affect the estimation of L_e. If the sky is clear the underestimation of L_e increases (Chason et al., 1991) compared to when it is cloudy. During my measurements the sky was always cloudy but sometimes the sky began to clear in the end of the measurements. This could have an impact when comparing L_e of different stands, where different sky conditions prevailed, with each other and have an impact on the relations between L_e and the vegetation indices and reflectance, but it is not possible to deduce anything about this from my results.

Since the relationships are empirical/statistical they are site specific and perhaps not applicable in other deciduous forests. The NDVI-LAI relationship varies seasonally and annually (Wang et al., 2005), which limits the use of the relationships obtained in this study. The relation is different during leaf production, leaf senescence and in the middle of the season when leaf area is constant (Wang et al., 2005). In this study the measurements were carried out in the end of the summer between August 16 and 1 October, and thus the relationships might not be applicable during the rest of the growing season. Even if measurements are conducted during the same phenological period the relationships might still not be the same another year because of changing environmental conditions between years (Wang et al., 2005). The SPOT image used in this study is from June 6, 2012 so both the phenological period and the year is different from when the measurements of L_e were conducted. The relationships are therefore probably different from what they would be if the measurements and satellite data were recorded at the same time.

The relationships between LAI and the vegetation indices obtained in this study could be used to estimate LAI on a large scale. This could be applied in environmental modeling, since LAI is related to the carbon balance of forests. Thus it can be used to estimate the potential of forests to act as carbon sinks to mitigate climate change.

6. Conclusions

The objective of this report was to identify any relations between optically estimated LAI, L_e, and vegetation indices/reflectance in deciduous forests.

From the results the following conclusions can be drawn:

- Good correlations were obtained for the relationships between L_e and VPI, NDVI, GEMI, EVI-2 and NIR reflectance for the estimated L_e values used in this study.
- The statistical relations are dependent on time and site specific conditions and might not be applicable in other environments. They might differ between seasons and years, which has been shown in earlier studies.
- The relationships can be used to get an estimate of LAI and to identify relative changes of LAI between different deciduous forests.
- The relations obtained for the vegetation indices depend on the relation between NIR reflectance and L_e. The red reflectance had a weak relation to L_e.

Overall my results show good potential for mapping LAI in deciduous forests on a large scale using simple linear relationships to the different vegetation indices of this study.

Acknowledgements

I want to thank my supervisor, Lars Eklundh, for his help and support during the course of this study and Hongxiao Jin for his help and useful comments on my results.
Thanks also to the SACCESS database for free SPOT data.

References

Asrar, G., M. Fuchs, E. T. Kanemasu, and J. L. Hatfield. 1984. Estimating absorbed photosynthetic radiation and leaf area index from spectral reflectance in wheat. *Agronomy Journal* 76: 300-306.

Astrium. 2013. Retrieved September 24, 2013, from http://www.astrium-geo.com/en/40-faq.

Black, T. A., J. M. Chen, X. Lee, and R. M. Sagar. 1991. Characteristics of shortwave and longwave irradiances under a Douglas-fir forest stand. *Canadian Journal of Forest Research* 21: 1020-1028.

Bausch, W. C. 1993. Soil background effects on reflectance-based crop coefficients for corn. *Remote Sensing of Environment* 46: 213– 222.

Ben-Ze'ev, E., A. Karnieli, N. Agam, Y. Kaufman, and B. Holben. 2006. Assessing vegetation condition in the presence of biomass burning smoke by applying the Aerosol-free Vegetation Index (AFRI) on MODIS images. *International Journal of Remote Sensing* 27: 3203–3221.

Chason, J. W., D. D. Baldocchi, and M. A. Huston. 1991. A comparison of direct and indirect methods for estimating forest canopy leaf area. *Agricultural and Forest Meteorology*, 57: 107-128.

Chen, J. M. and T. A. Black. 1992. Defining leaf area index for non-flat leaves. *Plant, Cell and Environment* 15: 421-429.

Cleugh, H. A., R. Leuning, Q. Mu, and S. W. Running. 2007. Regional evaporation estimates from flux tower and MODIS satellite data. *Remote Sensing of Environment* 106: 285–304.

Combal, B., F. Baret, M. Weiss, A. Trubuil, D. Macé, A. Pragnére, R. Myneni, Y. Knyazikhin, L. Wang. 2002. Retrieval of canopy biophysical variables from bidirectional reflectance Using prior information to solve the ill-posed inverse problem. *Remote Sensing of Environment* 84: 1 –15.

Cutini, A., G. Matteucci, and G. S. Mugnozza. 1998. Estimation of leaf area index with the Li-Cor LAI 2000 in deciduous forests. *Forest Ecology and Management* 105: 55–65.

Eklundh, L., K. Hall, H. Eriksson, J. Ardö, and P. Pilesjö. 2003. Investigating the use of Landsat thematic mapper data for estimation of forest leaf area index in southern Sweden. *Canadian Journal of Remote Sensing* 29:349-362.

Eriksson, H., L. Eklundh, K. Hall, and A. Lindroth. 2005. Estimating LAI in deciduous forest stands. *Agricultural and Forest Meteorology* 129: 27-37.

Eriksson, H. M., L. Eklundh, A. Kuusk, and T. Nilson. 2006. Impact of understory vegetation on forest canopy reflectance and remotely sensed LAI estimates. *Remote Sensing of Environment* 103: 408-418.

Houborg, R., H. Soegaard, and E. Boegh. 2007. Combining vegetation index and model inversion methods for the extraction of key vegetation biophysical parameters using Terra and Aqua MODIS reflectance data. *Remote Sensing of Environment* 106: 39-58.

Huete, A., K. Didan, T. Miura, E.P. Rodriguez, X. Gao, and L.G. Ferreira. 2002. Overview of the radiometric and biophysical performance of the MODIS vegetation indices. *Remote Sensing of Environment* 83: 195–213.

Liu, J., E. Pattey, and G. Jégo. 2012. Assessment of vegetation indices for regional crop green LAI estimation from Landsat images over multiple growing seasons. *Remote Sensing of Environment* 123: 347–358.

Miller, J. B. 1967. A formula for average foliage density. *Australian Journal of Botany* 15: 141-144.

Monteith, J. L. 1972. Solar radiation and productivity in tropical ecosystems. *Journal of Applied Ecology* 9: 747-766.

Rautiainen, M., P. Stenberg, T. Nilson, A. Kuusk, and H. Smolander. 2003.Application of a forest reflectance modelin estimating leaf area index of Scots pine stands using Landsat-7 TM reflectance data. *Canadian Journal of Remote Sensing* 29: 314-323.

Rocha, A.V. and G.R. Shaver. 2009. Advantages of a two band EVI calculated from solar and photosynthetically active radiation fluxes. *Agricultural and Forest Meteorology* doi:10.1016/j.agrformet.2009.03.016

SMHI – Swedish Meteorological and Hydrological Institute. 2014. Retrieved January 22, 2014, from www.smhi.se/klimatdata.

Soudani, K., C. François, G. le Maire, V. Le Dantec, and E. Dufrêne. 2006. Comparative analysis of IKONOS, SPOT, and ETM+ data for leaf area index estimation in temperate coniferous and deciduous forest stands. *Remote Sensing of Environment* 102: 161–175.

Tang, X., Z. Wang, J. Xie, D. Liu, A. R. Desai, M. Jia, Z. Dong, X. Liu, B. Liu. 2013. Monitoring the seasonal and interannual variation of the carbon sequestration in a temperate deciduous forest with MODIS time series data. *Forest Ecology and Management* 306: 150–160.

Turner, D. P., W. B. Cohen, R. E. Kennedy, K. S. Fassnacht, and J. M. Briggs. 1999. Relationships between leaf area index and Landsat TM spectral vegetation indices across three temperate zone sites. *Remote Sensing of Environment* 70: 52–68.

U.S. Geological Survey. 2011. Retrieved September 24, 2013, from http://eo1.usgs.gov/faq/question?id=21.

Wang, Q., S. Adiku, J. Tenhunen, and A. Granier. 2005. On the relationship of NDVI with leaf area index in a deciduous forest site. *Remote Sensing of Environment* 94: 244–255.

Waring, R. H. and G. B. Pitman. 1985. Modifying lodgepole pine stand of change susceptibility to mountain pine-beetle attack. *Ecology* 66: 889-897.

Appendix

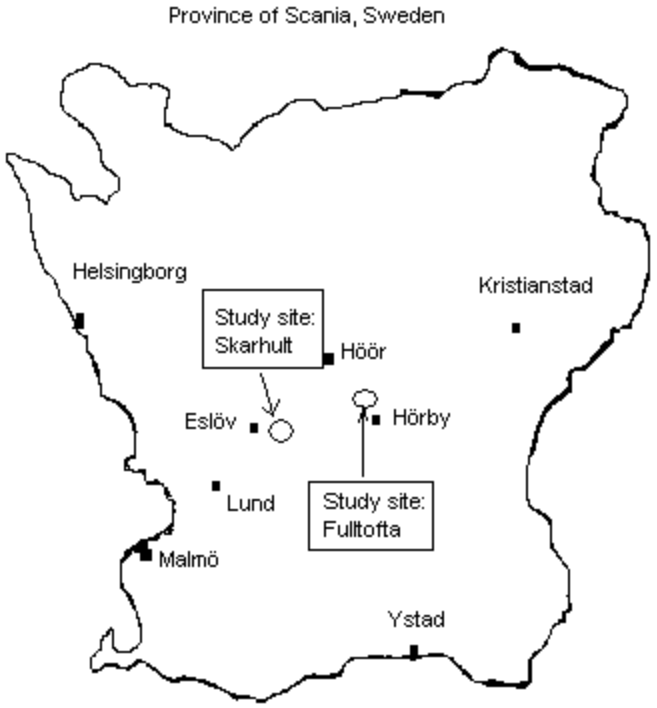

Figure 1. Study sites Skarhult and Fulltofta in the province of Scania, Sweden.

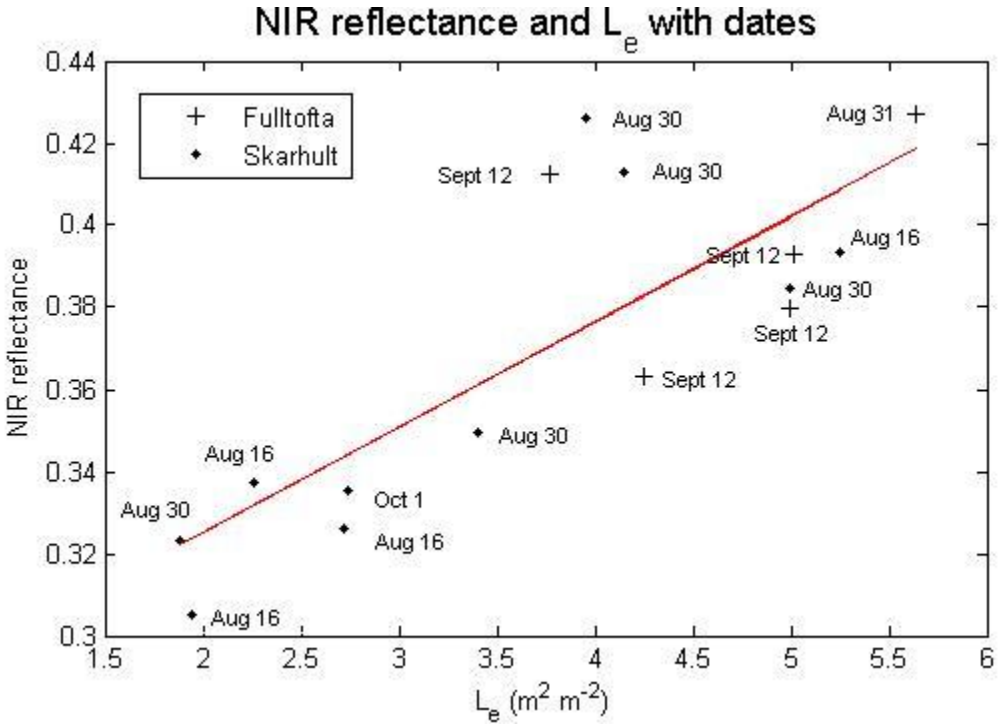

Figure 2. The relationship between NIR reflectance and L_e, with the dates in 2013 when measurements were carried out.

Institutionen för naturgeografi och ekosystemvetenskap, Lunds Universitet.

Student examensarbete (Seminarieuppsatser). Uppsatserna finns tillgängliga på institutionens geobibliotek, Sölvegatan 12, 223 62 LUND. Serien startade 1985. Hela listan och själva uppsatserna är även tillgängliga på LUP student papers (www.nateko.lu.se/masterthesis) och via Geobiblioteket (www.geobib.lu.se)

The student thesis reports are available at the Geo-Library, Department of Physical Geography and Ecosystem Science, University of Lund, Sölvegatan 12, S-223 62 Lund, Sweden. Report series started 1985. The complete list and electronic versions are also electronic available at the LUP student papers (www.nateko.lu.se/masterthesis) and through the Geo-library (www.geobib.lu.se)

245 Linnea Jonsson (2012). Impacts of climate change on Pedunculate oak and Phytophthora activity in north and central Europe
246 Ulrika Belsing (2012) Arktis och Antarktis föränderliga havsistäcken
247 Anna Lindstein (2012) Riskområden för erosion och näringsläckage i Segeåns avrinningsområde
248 Bodil Englund (2012) Klimatanpassningsarbete kring stigande havsnivåer i Kalmar läns kustkommuner
249 Alexandra Dicander (2012) GIS-baserad översvämningskartering i Segeåns avrinningsområde
250 Johannes Jonsson (2012) Defining phenology events with digital repeat photography
251 Joel Lilljebjörn (2012) Flygbildsbaserad skyddszonsinventering vid Segeå
252 Camilla Persson (2012) Beräkning av glaciärers massbalans – En metodanalys med fjärranalys och jämviktslinjehöjd över Storglaciären
253 Rebecka Nilsson (2012) Torkan i Australien 2002-2010 Analys av möjliga orsaker och effekter
254 Ning Zhang (2012) Automated plane detection and extraction from airborne laser scanning data of dense urban areas
255 Bawar Tahir (2012) Comparison of the water balance of two forest stands using the BROOK90 model
256 Shubhangi Lamba (2012) Estimating contemporary methane emissions from tropical wetlands using multiple modelling approaches
257 Mohammed S. Alwesabi (2012) MODIS NDVI satellite data for assessing drought in Somalia during the period 2000-2011
258 Christine Walsh (2012) Aerosol light absorption measurement techniques: A comparison of methods from field data and laboratory experimentation
259 Jole Forsmoo (2012) Desertification in China, causes and preventive actions in modern time
260 Min Wang (2012) Seasonal and inter-annual variability of soil respiration at Skyttorp, a Swedish boreal forest
261 Erica Perming (2012) Nitrogen Footprint vs. Life Cycle Impact Assessment methods – A comparison of the methods in a case study.
262 Sarah Loudin (2012) The response of European forests to the change in

summer temperatures: a comparison between normal and warm years, from 1996 to 2006

263 Peng Wang (2012) Web-based public participation GIS application – a case study on flood emergency management

264 Minyi Pan (2012) Uncertainty and Sensitivity Analysis in Soil Strata Model Generation for Ground Settlement Risk Evaluation

265 Mohamed Ahmed (2012) Significance of soil moisture on vegetation greenness in the African Sahel from 1982 to 2008

266 Iurii Shendryk (2013) Integration of LiDAR data and satellite imagery for biomass estimation in conifer-dominated forest

267 Kristian Morin (2013) Mapping moth induced birch forest damage in northern Sweden, with MODIS satellite data

268 Ylva Persson (2013) Refining fuel loads in LPJ-GUESS-SPITFIRE for wet-dry areas - with an emphasis on Kruger National Park in South Africa

269 Md. Ahsan Mozaffar (2013) Biogenic volatile organic compound emissions from Willow trees

270 Lingrui Qi (2013) Urban land expansion model based on SLEUTH, a case study in Dongguan City, China

271 Hasan Mohammed Hameed (2013) Water harvesting in Erbil Governorate, Kurdistan region, Iraq - Detection of suitable sites by using Geographic Information System and Remote Sensing

272 Fredrik Alström (2013) Effekter av en havsnivåhöjning kring Falsterbohalvön.

273 Lovisa Dahlquist (2013) Miljöeffekter av jordbruksinvesteringar i Etiopien

274 Sebastian Andersson Hylander (2013) Ekosystemtjänster i svenska agroforestrysystem

275 Vlad Pirvulescu (2013) Application of the eddy-covariance method under the canopy at a boreal forest site in central Sweden

276 Malin Broberg (2013) Emissions of biogenic volatile organic compounds in a Salix biofuel plantation – field study in Grästorp (Sweden)

277 Linn Renström (2013) Flygbildsbaserad förändringsstudie inom skyddszoner längs vattendrag

278 Josefin Methi Sundell (2013) Skötseleffekter av miljöersättningen för natur- och kulturmiljöer i odlingslandskapets småbiotoper

279 Kristín Agustsdottír (2013) Fishing from Space: Mackerel fishing in Icelandic waters and correlation with satellite variables

280 Cristián Escobar Avaria (2013) Simulating current regional pattern and composition of Chilean native forests using a dynamic ecosystem model

281 Martin Nilsson (2013) Comparison of MODIS-Algorithms for Estimating Gross Primary Production from Satellite Data in semi-arid Africa

282 Victor Strevens Bolmgren (2013) The Road to Happiness – A Spatial Study of Accessibility and Well-Being in Hambantota, Sri Lanka

283 Amelie Lindgren (2013) Spatiotemporal variations of net methane emissions and its causes across an ombrotrophic peatland - A site study from Southern Sweden

284 Elisabeth Vogel (2013) The temporal and spatial variability of soil respiration in boreal forests - A case study of Norunda forest, Central Sweden

285 Cansu Karsili (2013) Calculation of past and present water availability in the Mediterranean region and future estimates according to the Thornthwaite water-balance model
286 Elise Palm (2013) Finding a method for simplified biomass measurements on Sahelian grasslands
287 Manon Marcon (2013) Analysis of biodiversity spatial patterns across multiple taxa, in Sweden
288 Emma Li Johansson (2013) A multi-scale analysis of biofuel-related land acquisitions in Tanzania - with focus on Sweden as an investor
289 Dipa Paul Chowdhury (2013) Centennial and Millennial climate-carbon cycle feedback analysis for future anthropogenic climate change
290 Zhiyong Qi (2013) Geovisualization using HTML5 - A case study to improve animations of historical geographic data
291 Boyi Jiang (2013) GIS-based time series study of soil erosion risk using the Revised Universal Soil Loss Equation (RUSLE) model in a micro-catchment on Mount Elgon, Uganda
292 Sabina Berntsson & Josefin Winberg (2013) The influence of water availability on land cover and tree functionality in a small-holder farming system. A minor field study in Trans Nzoia County, NW Kenya
293 Camilla Blixt (2013) Vattenkvalitet - En fältstudie av skånska Säbybäcken
294 Mattias Spångmyr (2014) Development of an Open-Source Mobile Application for Emergency Data Collection
295 Hammad Javid (2013) Snowmelt and Runoff Assessment of Talas River Basin Using Remote Sensing Approach
296 Kirstine Skov (2014) Spatiotemporal variability in seasonal methane emission from an Arctic fen – dynamics and driving factors
297 Sandra Persson (2014) Estimating leaf area index from satellite data in deciduous forests of southern Sweden